

Searches for Supersymmetry at CMS using the 2010 Data

C. Bernet, on behalf of the CMS collaboration
CERN, Geneva.

Searches for supersymmetry were conducted using the 35 pb^{-1} of data collected by the CMS experiment at the LHC in 2010, at a centre-of-mass energy of 7 TeV. A wide variety of final states featuring jets and missing transverse energy, possibly with leptons, were investigated. The data, consistent with the standard-model hypothesis, allow us to set limits on the existence of new physics, extending those previously obtained at the Tevatron and LEP.

1 Introduction

The standard model (SM) of particle physics has been enormously successful in describing all phenomena at the highest attainable energies thus far. Yet, it is widely believed to be only an effective description of a more complete theory which is valid at the highest energy scales. Of particular theoretical interest is supersymmetry (SUSY)^{1 2 3 4 5} which solves the hierarchy problem^{6 7} of the SM by compensating for each of the fermionic and bosonic degrees of freedom in the SM with a supersymmetric bosonic and fermionic degree of freedom, respectively. The resulting superfields have the same quantum numbers as their SM counterparts, except for spin. Since no SUSY particle has been observed so far, they must have higher masses than their SM partners, implying that SUSY is a broken symmetry.

At the Large Hadron Collider (LHC) at CERN, supersymmetric particles, if they exist, are predicted to be produced dominantly via QCD, through the fusion of two gluons into a pair of gluinos, a pair of squarks, or a gluino and a squark. The production cross-section for massive squarks or gluinos falls as a power law with the squark or gluino mass, following the available energy \sqrt{s} in the partonic centre-of-mass frame. The LHC, with a proton-proton centre-of-mass energy \sqrt{s} of 7 TeV, is a copious source of high-energy partons which allows to probe squark and gluino masses beyond the limits previously set at LEP and at the Tevatron. Squarks and gluinos initiate a decay cascade in which quarks are produced, until the lightest supersymmetric particle (LSP) is created. The dynamics of the cascade depends on the SUSY model under consideration, and in particular on the masses of the supersymmetric particles. If R-parity is conserved, the LSP is unable to decay into SM particles and is therefore stable. If, in addition, the LSP is a neutralino, it is weakly interacting and thus escapes detection, hence missing transverse energy (E_T^{miss}) in the final state. Typical hadronic decay modes for gluinos (\tilde{g}) and squarks (\tilde{q}) are $\tilde{q} \rightarrow q\chi_1^0$ and $\tilde{g} \rightarrow qq\chi_1^0$. In these examples, the squark and the gluino directly decay to the lightest neutralino χ_1^0 , the gluino doing so via an off-shell squark. As a result, squark pair production usually gives rise to more than two jets, and gluino pair production to more than four jets. The transverse momenta of the jets are driven by the difference in mass between the squark or gluino and the neutralino. Leptons can appear in the final state, for example if heavy neutralinos ($\tilde{\chi}_2^0 \rightarrow l^\pm \tilde{l}^\mp \rightarrow l^\pm l^\mp \chi_1^0$) or charginos ($\tilde{\chi}_1^\pm \rightarrow \chi_1^0 W^\pm$) are created in

the decays cascades of the squark or gluino.

The CMS detector⁸ is used to investigate many final states that could arise from the strong production of squarks and gluinos. An effort is made to make these final states independent, so that all analyses can ultimately be easily combined. Because the presence of leptons is not guaranteed, investigating hadronic final states with jets and high missing transverse energy is the most efficient way to look for SUSY. Dealing with the huge QCD background is however a challenge. In CMS, three complementary approaches are followed. The α_T analysis, presented elsewhere⁹ makes use of the α_T variable to completely remove the QCD background from the search region, leaving solely electroweak backgrounds, namely $t\bar{t} + jets$, $W + jets$ and $Z \rightarrow \nu\nu + jets$. The jets + H_T^{miss} analysis, summarized in Section 2.1, consists of looking for an excess of multi-jet events at high H_T^{miss} , an approximation of the E_T^{miss} computed as the opposite of the vector sum of the jet transverse momenta. This approach is the most efficient of the three, but requires the QCD background to be accurately controlled. The so-called razor analysis, presented in Section 2.2 relies on novel variables to reduce the QCD background to a negligible level in the search region, and to predict the background contribution. The final search sample of this analysis has about 30% of events in common with the jets + H_T^{miss} analysis. While the razor analysis is less efficient than the jets + H_T^{miss} analysis, it is less sensitive to the effects of initial state radiation. Requiring leptons in the final state in addition to jets and missing transverse energy strongly reduce the standard-model background. With one isolated lepton, the QCD and $Z \rightarrow \nu\nu + jets$ backgrounds get suppressed. With two opposite-sign leptons¹⁰, the $W + jets$ background becomes negligible, and several handles can be used for an accurate estimation of the remaining $t\bar{t}$ background from the data. Asking for two same-sign leptons, or for three or more leptons, dramatically suppresses the standard-model background, for a very clean search of physics beyond the standard model, like the production of squarks and gluinos which can naturally lead to such final states.

In these proceedings, the emphasis is put on the most recent fully hadronic analyses, and several leptonic analyses are briefly summarized. Other important search fields are also being covered by CMS but could not be presented here. For example, in the context of the general gauge-mediated SUSY breaking with the lightest neutralino as the next-to-lightest supersymmetric particle and the gravitino as the lightest, a natural signature for squark or gluino production is the presence of two photons and E_T^{miss} in the final state¹¹.

2 Fully hadronic searches

2.1 Jets + H_T^{miss} analysis

The data used in this analysis¹² are collected using triggers requiring a minimal jet activity H_T^{trig} , measured as the scalar sum of the transverse momentum of the calorimeter jets reconstructed at trigger level. The rapid increase in instantaneous luminosity during the 2010 data taking resulted in the threshold on H_T^{trig} being raised from 100 to 140 and finally 150 GeV. The particle flow algorithm^{13 14} identifies and reconstructs all particles produced in the collision, namely charged hadrons, photons, neutral hadrons, muons, and electrons. The resulting list of particles is then used to reconstruct particle jets, compute the E_T^{miss} , and quantify the lepton isolation.

The event selection starts from a loose validation region. On top of this baseline selection, tighter selection criteria are applied to define the search regions. The baseline selection requirements after trigger boil down to selecting events with (i) at least three jets with $p_T > 50$ GeV/c and $\eta < 2.5$; (ii) $H_T > 300$ GeV, where H_T is defined as the scalar sum of the transverse momenta of all the jets having $p_T > 50$ GeV/c and $\eta < 2.5$; (iii) $H_T^{\text{miss}} > 150$ GeV, where H_T^{miss} is defined as the magnitude of the vectorial sum of the p_T of the jets having, in this case, $p_T > 30$ GeV/c and $\eta < 5$; (iii) no isolated electron nor muon with $p_T > 10$ GeV/c. Additionally,

the H_T^{miss} vector is required not to be aligned with one of the three leading jets, to reject QCD multi-jet events in which a single mis-measured jet yields high H_T^{miss} .

Two search regions were defined in this inclusive jets-plus-missing-momentum search. The first search selection, defining the “high- H_T^{miss} search region”, tightens the baseline cuts with an $H_T^{\text{miss}} > 250$ GeV requirement, to search for a generic invisible particle in a low background environment. The second selection adds a $H_T > 500$ GeV cut to the baseline selection, yielding the “high- H_T search region”, sensitive to cascade decays of high-mass new-physics particles where more energy is transferred to visible particles and less to the dark-matter candidate. The main background contributions in the two search regions are estimated using data-driven techniques. Due to its huge cross-section, QCD multi-jet production can give rise to high H_T^{miss} because of the finite jet energy resolution, or of rare but dramatic mis-measurements of the jet energy induced by various instrumental effects. The most important instrumental effects were identified in the simulation to be related to missing channels in the ECAL, and to jet punch-through giving rise to multi-TeV fake muons in the particle jets. The simulation was used to design dedicated event filters to remove such events.

The QCD background was estimated using the so-called “rebalance+smear” technique. An inclusive multi-jet sample of events is selected. The energy of each jet is first rescaled to obtain a null H_T^{miss} using a maximum-likelihood fit taking into account the jet energy resolution in the process. This rescaling produces a seed event from which all sources of H_T^{miss} , possibly genuine, have been removed. The jets are then smeared by a simulated jet energy response distribution. The simulated distribution is corrected for differences between the data and the simulation by factors obtained from di-jet asymmetry measurements. The other standard-model background events contributing to the search regions feature at least one neutrino in the final state, hence true H_T^{miss} . W+jets events, where the W possibly comes from a top and decays to a lepton and a neutrino, end up in the search region in case the lepton from the W decay is not identified in the analysis, either because it is a τ decaying hadronically, or an electron or muon that is lost (not identified by the lepton veto). The contribution of this source of background is estimated by selecting from the data a control sample of events with an isolated muon and jets. To predict the number of events with a lost lepton in the search region, the number of events in this control sample is corrected for lepton reconstruction and identification efficiency by factors measured using Z events in the data, and by acceptance factors from the simulation. To estimate the number of events in which a tau decays hadronically, the muon in the control sample is replaced by a jet representing the hadronically decaying tau, which is taken into account when applying the search selections. The uncertainty on the W+jets background estimation (including $t\bar{t}$) is dominated by the statistical error on the number of events in the control sample. The last source of background, especially important because it dominates at high H_T^{miss} , is $Z \rightarrow \nu\nu$ +jets. As no $Z \rightarrow ee$ nor $Z \rightarrow \mu\mu$ events are observed in the search regions, these processes cannot be used to predict the $Z \rightarrow \nu\nu$ +jets background contribution. This contribution is instead estimated using a control sample of isolated γ +jets events, in which the photon is ignored when applying the search selections. This strategy exploits the fact that at high boson p_T , the Z and γ behave in a similar way, apart from electroweak coupling differences, and small residual mass effects. The number of events in the control sample is corrected by a Z γ cross-section correction factor obtained from the simulation. Several other effects, such as the contamination of the control sample by multi-jet QCD events, or the photon reconstruction and identification efficiencies, are taken into account. The error on this background prediction comes from the statistical error on the number of events in the control sample, and from systematic errors mostly related to the available number of events in the simulated samples and to the estimation of the contamination of the control sample by multi-jet events. Table 1 summarizes the results of the analysis, and shows that no excess of events is found in the data. The limit set on the number of signal events is interpreted in the context of various SUSY models in Section 2.3.

Table 1: Predicted and observed event yields for the baseline selection, and for the high- H_T^{miss} and high- H_T search selections. The last line reports the 95% CL limit on the number of signal events given the observed number of events, and the total predicted background.

Background	Baseline selection	High- H_T^{miss} selection	High- H_T selection
$Z \rightarrow \nu\nu + jets$ (γ +jets method)	26.3 \pm 4.8	7.1 \pm 2.2	8.4 \pm 2.3
$W t\bar{t} \rightarrow e \mu + X$	33.0 \pm 8.1	4.8 \pm 1.9	10.9 \pm 3.4
$W t\bar{t} \rightarrow \tau_{\text{had}} + X$	22.3 \pm 4.6	6.7 \pm 2.1	8.5 \pm 2.5
QCD	29.7 \pm 15.2	0.16 \pm 0.10	16.0 \pm 7.9
Total background estimated from data	111.3 \pm 18.5	18.8 \pm 3.5	43.8 \pm 9.2
Observed in 36 pb $^{-1}$ of data	111	15	40
95% C.L. limit on signal events	40.4	9.6	19.6

2.2 Razor analysis

This analysis relies on the novel “razor” variables¹⁵ to define search regions and predict the background contribution in a data-driven way. For the pair-production of two heavy particles of mass $M_{\tilde{q}}$ decaying into a visible part and an invisible part of mass M_{χ} , the variable M_R provides an approximation of the quantity $M_{\Delta} \equiv (M_{\tilde{q}}^2 - M_{\chi}^2) M_{\tilde{q}}$. The search consists of looking for a signal peak in the M_R distribution, on top of a steeply falling standard-model background distribution. Cutting on the dimensionless R variable strongly reduces the standard-model background, and to give its M_R distribution an easy-to-control exponential shape.

The razor analysis¹⁶ defines a set of physics objects, namely jets, isolated electrons, and isolated muons. All of these objects are used in the computation of R and M_R , which proceeds in the following way. The objects are first grouped into two “mega-jets” using an hemisphere algorithm. Each mega-jet ideally corresponds to the visible part of the decay products of one of the pair-produced heavy particles. The R and M_R variables are then computed using the 4-momenta of the two mega-jets, and the E_T^{miss} vector. Depending on the presence of an isolated electron or muon in the final states, the events are classified in three independent “boxes”, the electron box, the muon box, and the hadronic box. The high R , high M_R region of each box constitutes an independent search region. The razor analysis is thus both a fully hadronic and a single lepton analysis. In these proceedings however, the focus is put on the more efficient fully hadronic sector, for which the low- M_R region of the leptonic boxes is used as a control sample

The event sample was collected using triggers based on the presence of a single electron, a single muon, and on H_T^{trig} . The jets are required to have $p_T > 30$ GeV/ c and $|\eta| < 3$, electrons to have $p_T > 20$ GeV/ c and $|\eta| < 2.5$, and muons to have $p_T > 20$ GeV/ c and $|\eta| < 2.1$. The difference in azimuth between the two mega-jets is required to be smaller than 2.8 rad, to reject di-jet QCD events. The M_R distribution for the data in the hadronic box, together with the full background prediction, is shown in Fig. 1, for $R > 0.5$.

The background prediction is based on the observation that above a given

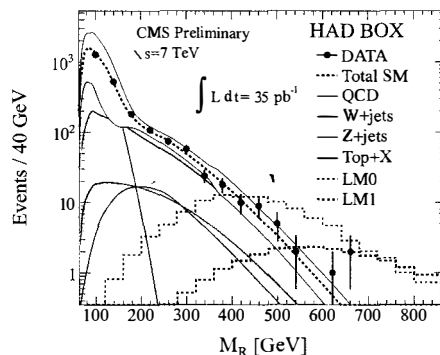


Figure 1: Distribution of M_R in the data, and background prediction for the “razor” analysis, with $R > 0.5$. The search region is defined by the additional requirement $M_R > 500$ GeV/ c^2 .

value of M_R , all background distributions drop following an exponential function. At low M_R , the background shape is mostly driven by the efficiency of the H_T trigger, and by the mass scales of the standard-model processes. For instance, M_R peaks around the mass of the top quark for $t\bar{t}$ events.

For the $t\bar{t}$, $Z \rightarrow \nu\nu$ +jets, and W+jets backgrounds, the parameters of the exponential function driving the evolution of the M_R distribution at high M_R are taken from the simulation. In the simulation, and also in Fig. 1, these parameters appear to be roughly equal, indicating a similar behaviour of these background processes in terms of R and M_R . These parameters are then corrected by factors compatible with one, extracted from a comparison between data and simulation for W+jets events in the muon box. The relative normalization of these three sources of background is set according to the inclusive W, Z, and $t\bar{t}$ cross-sections measured by CMS^{17 18}. The normalization of the overall background distribution to the data is performed by measuring lepton boxes event yields, which are then corrected for lepton reconstruction and identification efficiency. A fit is finally performed in the $80 < M_R < 400$ GeV/ c^2 region, to obtain the parameters of the H_T trigger turn-on shape and the overall normalization of the QCD background. The shape of the QCD background was obtained using a low-bias, prescaled trigger. The background is predicted by extrapolating the resulting background distribution to the search region, defined as $M_R > 500$ GeV/ c^2 . In this region, 7 events are observed in the data, and 5.5 ± 1.4 are expected from the background. As no excess is observed, a model-independent upper limit is set on the number of signal events, $s < 8.4$. This limit is interpreted in the context of various SUSY models in Section 2.3.

2.3 Model dependent interpretation

The results of the fully hadronic (Sections 2.1 and 2.2) analyses were interpreted in the context of the constrained MSSM (cMSSM), a truncation of the full parameter space of the MSSM motivated by the minimal supergravity framework for spontaneous soft breaking of supersymmetry. In the cMSSM, the soft breaking parameters are reduced to five: three mass parameters, m_0 , $m_{1/2}$ and A_0 being respectively the universal scalar mass, the universal gaugino mass, and the universal trilinear scalar coupling, as well as $\tan\beta$, the ratio of the up-type and down-type Higgs vacuum expectation values, and the sign of the supersymmetric Higgs mass parameter μ . Scanning over this parameter space yields models which, while not entirely representative of the complete MSSM, vary widely in their supersymmetric mass spectra and thus in the dominant production channels and decay chains.

After fixing A_0 , $\tan\beta$ and the sign of μ , the model independent upper limit s^* on the number of signal events s from each analysis is projected on the $(m_0, m_{1/2})$ plane by excluding the model if $s(m_0, m_{1/2}) > s^*$. The various sources of uncertainty on the signal yield and the signal contamination of the control samples are taken into account. Figures 2(a) and (b) present the limits set by the jets+ H_T^{miss} and razor analyses. The expected limits are obtained by taking the median of the background test statistics as the result of the experiment, and the $\pm 1\sigma$ band by taking the median $\pm 1\sigma$.

The results of the fully hadronic analyses were also interpreted in the context of two benchmark simplified models¹⁹: gluino-LSP production (left) and squark-LSP production (right). The former refers to pair-produced gluinos, where each gluino directly decays to two light quarks and the LSP resulting in a four jet plus missing transverse energy final state. The latter refers to pair-produced squarks, where each squark decays to one jet and the LSP resulting in a two jet plus missing transverse energy final state. Figures 2(c) and (d) show the upper limit on the cross-section as a function of the physical masses of the particles involved in each model. In each bin, the upper limits obtained in the α_T , the jets+ H_T^{miss} and the razor analyses are considered, and the minimum one is shown. Theoretical uncertainties are not included.

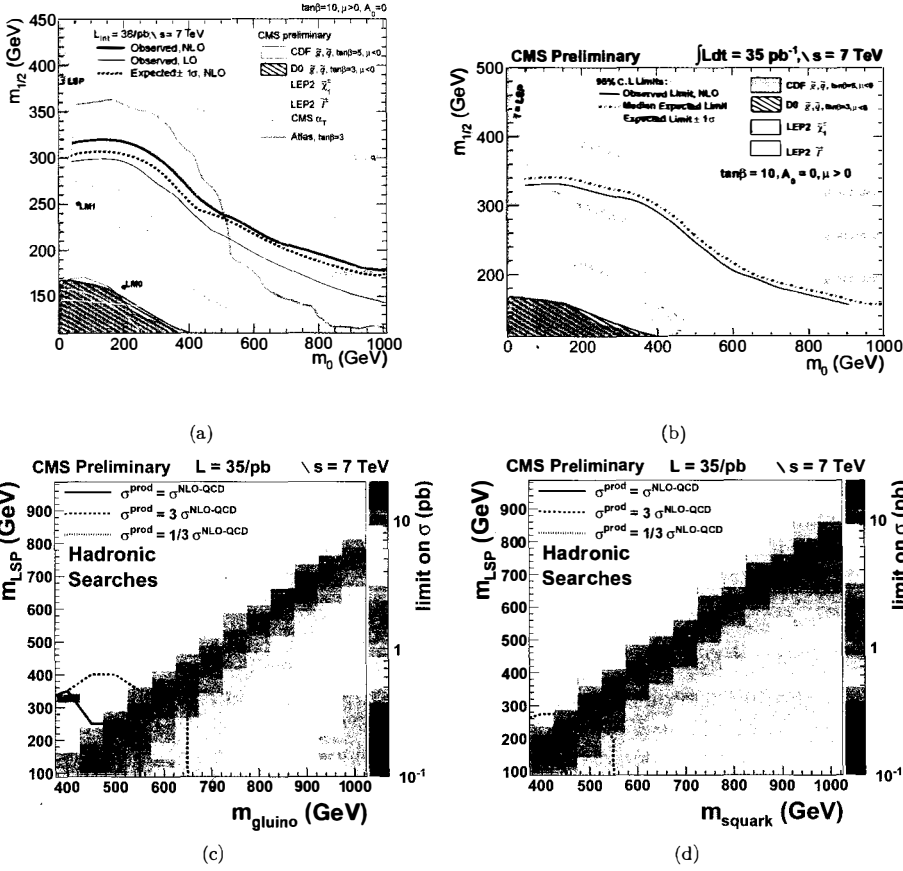


Figure 2: Expected and observed 95% C.L. limits in the cMSSM (m_0 $m_{1/2}$) parameter plane for (a) the jets+ H_T^{miss} analysis and (b) the razor analysis. Limits on the di-gluino (c) and di-squark (d) cross-sections in simplified models, obtained by combining the three fully hadronic analyses, namely α_T , jets+ H_T^{miss} and razor.

3 Leptonic searches

The single lepton analysis²⁰ selects events featuring jets, E_T^{miss} , and a single lepton in the final state. The presence of the lepton strongly reduces the contribution of the QCD multi-jet and $Z \rightarrow \nu\nu$ +jets backgrounds, and provides several handles to build a data-driven prediction of the remaining background contribution from QCD, $t\bar{t}$, and W +jets. Events containing an additional lepton are vetoed, and handled by the di-lepton and multi-lepton analyses. The event sample was collected using triggers based on the presence of a single electron or a single muon. The requirement of an H_T trigger was added when the peak luminosity increased beyond $2 \times 10^{32} \text{ cm}^{-2} \text{ s}^{-1}$. The trigger selection is fully efficient with respect to the baseline selection applied offline, which consists of requiring (i) four jets with $p_T > 30 \text{ GeV}/c$ and $\eta < 2.4$ with $H_T > 500 \text{ GeV}$; (ii) an isolated lepton, which can be either a muon with $p_T > 20 \text{ GeV}/c$ and $\eta < 2.1$, or an electron with $p_T > 20 \text{ GeV}/c$ and $\eta < 2.4$. The search region is defined by an additional cut on the missing transverse energy, $E_T^{\text{miss}} > 250 \text{ GeV}$. The contribution of the

main background processes to the search region, $t\bar{t}$ and W +jets, is estimated using the lepton spectrum method. The foundation of this method is that, when the lepton and neutrino are produced together in a W decay (either in $t\bar{t}$ or in W +jets events), the lepton p_T spectrum is directly related to the neutrino p_T spectrum. The lepton spectrum is used to predict the E_T^{miss} distribution, after suitable corrections related to the effect of the W polarisation on the lepton and neutrino p_T spectra, and to the lepton acceptance and reconstruction efficiency. Combining the electron and muon channels, 2 events are observed in the search region, while 3.6 ± 2.9 are expected. A 95% model independent upper limit of 4.1 signal events is calculated. In the cMSSM, for $\tan\beta = 10$, $A_0 = 0$, and $\mu > 0$, gluino and squark masses larger than about $550 \text{ GeV}/c^2$ are excluded.

The same-sign di-lepton analysis requires, in addition to jets and E_T^{miss} , exactly two isolated leptons of the same sign which can be electrons, muons or taus decaying hadronically. The event sample was collected using di-lepton and single-lepton triggers, but also H_T triggers, which provide sensitivity to events with low p_T electrons and muons. The search selection and the data-driven background estimation techniques employed were chosen according to the trigger in use (lepton or hadron), and the channel ($l_i l_j$ where $l_{i,j} = e, \mu, \tau$). In all search regions, the predicted number of background events is compatible with zero, and no excess is observed. The analysis and the results are described in details in Ref²¹, which also provides lepton efficiency maps that can be used to test a variety of models.

The multi-lepton analysis²² selects events with three isolated leptons or more, acquired using single-lepton and di-lepton triggers. The events are sorted in 54 independent samples according to the relative charge of the leptons and their flavour, which can be e, μ , and τ . The three-lepton requirement strongly reduces the standard-model background, and the largest remaining background process is Z +jets, including Drell-Yan. The remaining background is further suppressed by requiring $H_T > 30 \text{ GeV}$, $E_T^{\text{miss}} > 50 \text{ GeV}$ or a Z veto, depending on the considered final state. No excess is found with respect to the predicted background in search region, and limits are set in a variety of models. In particular, in the so-called co-NLSPs scenario (see Ref²³ and references therein), squark and gluino masses lower than $830 \text{ GeV}/c^2$ and $1040 \text{ GeV}/c^2$ are excluded.

4 Conclusion

Complementary searches for Supersymmetry and other new physics leading to similar final states were conducted at CMS using the 35 pb^{-1} of data collected in 2010, in a wide variety of final states. No excess has been observed so far with respect to the expectations from the standard model, and stringent limits were set in various SUSY models. Data-driven background estimation techniques have been used wherever possible, paving the way towards the analysis of high-luminosity 2011 data.

5 Acknowledgements

I would like to thank the members of the CMS collaboration for the excellent performance of the detector and of all the steps culminating in these results, as well as the members of the CERN accelerator departments for the smooth operation of the LHC machine.

1. J. Wess and B. Zumino. Supergauge transformations in four dimensions. *Nucl. Phys.*, B70:39, 1974.
2. H.P.Nilles. Supersymmetry, supergravity and particle physics. *Phys. Reports*, 110:1, 1984.
3. H. E. Haber and G. L. Kane. The search for supersymmetry: Probing physics beyond the standard model. *Phys. Reports*, 117:75, 1987.

4. S. Ferrara R. Barbieri and C. A. Savoy. Gauge models with spontaneously broken local supersymmetry. *Phys. Lett.*, B 119:343, 1982.
5. E. Eichten S. Dawson and C. Quigg. Search for supersymmetric particles in hadron-hadron collisions. *Phys. Rev.*, D31:1581, 1985.
6. E.Witten. Dynamical breaking of supersymmetry. *Nucl. Phys.*, B 188:513, 1981.
7. S.Dimopoulos and H.Georgi. Softly broken supersymmetry and SU(5). *Nucl. Phys.*, B 193:150, 1981.
8. The CMS experiment at the CERN LHC. *JINST*, 0803:S08004, 2008.
9. The CMS collaboration. Search for supersymmetry in pp collisions at 7 TeV in events with jets and missing transverse energy. oai:cds.cern.ch:1320934. 2011.
10. The CMS collaboration. Search for physics beyond the standard model in opposite-sign dilepton events in pp collisions at $\sqrt{s} = 7$ TeV. oai:cds.cern.ch:1333985. 2011.
11. The CMS collaboration. Search for supersymmetry in pp collisions at $\sqrt{s} = 7$ TeV in events with two photons and missing transverse energy. *To appear*, 2011.
12. The CMS collaboration. Search for new physics at CMS with jets and missing momentum. *CMS PAS*, SUS-10-005, 2011.
13. The CMS collaboration. Particle-flow event reconstruction in CMS and performance for jets, taus, and missing E_T . *CMS PAS*, PFT-09-001, 2009.
14. The CMS collaboration. Commissioning of the particle-flow reconstruction in minimum-bias and jet events from pp collisions at 7 TeV. *CMS PAS*, PFT-10-002, 2010.
15. C. Rogan. Kinematics for new dynamics at the LHC. arxiv:1006.2727v2 [hep-ph]. *CALT 68-2790*, 2010.
16. The CMS collaboration. Inclusive search for squarks and gluinos at $\sqrt{s} = 7$ TeV. *CMS PAS*, SUS-10-009, 2011.
17. Measurements of inclusive w and z cross sections in pp collisions at 7 TeV. *CMS PAS*, EWK-10-002, 2010.
18. The CMS collaboration. Selection of top-like events in the dilepton and lepton-plus-jets channels in early 7 TeV data. *CMS PAS*, TOP-10-004, 2010.
19. Johan Alwall, Philip Schuster, and Natalia Toro. Simplified models for a first characterization of new physics at the LHC. *Phys.Rev.*, D79:075020, 2009.
20. The CMS collaboration. Search for supersymmetry in proton-proton collisions at $\sqrt{s} = 7$ TeV in events with a single lepton, jets, and missing transverse momentum. *CMS PAS*, SUS-10-006, 2011.
21. The CMS collaboration. Search for new physics with same-sign isolated dilepton events with jets and missing transverse energy at the LHC. arxiv:cds.cern.ch:1345080. 2011.
22. The CMS collaboration. Search for physics beyond the standard model using multilepton signatures in $\sqrt{s} = 7$ TeV pp collisions with the CMS detector at the LHC. *To appear*, 2011.
23. Joshua T. Ruderman and David Shih. Slepton co-NLSPs at the Tevatron. arxiv:1009.1665 [hep-ph]. 2010.